Hygrothermomechanical Evaluation of Transverse Filament Tape Epoxy/Polyester Fiberglass Composites

R. L. Lark and C. C. Chamis
Lewis Research Center
Cleveland, Ohio

NASA

HYGROTHERMOMECHANICAL EVALUATION OF TRANSVERSE FILAMENT TAPE EPOXY/POLYESTER FIBERGLASS COMPOSITES

R. F. Lark[*] and C. C. Chamis[**]

National Aeronautics and Space Administration
Lewis Research Center
Cleveland, Ohio 44135

ABSTRACT

The static and cyclic load behavior of transverse filament tape (TFT) fiberglass/epoxy and TFT fiberglass/polyester composites, intended for use in the design of low-cost wind turbine blades, are presented. The data behavior is also evaluated with respect to predicted properties based on an integrated hygrothermomechanical response theory.

Experimental TFT composite data were developed by the testing of laminates made by using composite layups typical of those used for the fabrication of TFT fiberglass wind turbine blades. Static properties include tension, compression, and interlaminar shear strengths at ambient conditions and at high humidity/elevated temperature conditions after a 500 hour exposure. Cyclic fatigue data were obtained using similar environmental conditions and a range of cyclic stresses.

The environmental (temperature and moisture) and cyclic load effects on composite strength degradation are subsequently compared with the predictions obtained by using the composite life/durability theory developed at NASA-Lewis. The results obtained show that the predicted hygrothermomechanical environmental effects on TFT composites are in good agreement with measured data for various properties including fatigue at different cyclic stresses. The results obtained also demonstrate that the integrated hygrothermomechanical and fatigue life theories can be used to analyze and assess TFT composites with relatively little experimental data.

1.0 INTRODUCTION

The objective of this paper is to compare the experimental and predicted static and cyclic fatigue properties of both transverse filament tape (TFT) TFT/epoxy and TFT/polyester composites. The experimental data were developed by the testing of flat TFT lamintes made by using composite layups typical of those used for the fabrication of TFT fiberglass wind turbine blades. Static properties developed include tension, compression, and interlaminar shear strengths at ambient room condition and at high humidity/elevated temperature conditons after a 500 hour exposure. Cyclic fatigue data were obtained using similar environmental conditons over a range of R-ratios (max. to min. cyclic applied stress). The experimental fiberglass TFT data summarized in this report were obtained under a Department of Energy/NASA-Lewis Research Center program (ref. 1).

---

[*] Aerospace Engineer.
[**] Aerospace Structures and Composites Engineer.

The degradation effects of both moisture and temperature on the properties of TFT composites were analyzed by using an integrated theory to predict the hygrothermomechanical response of advanced fiber composite laminates The theory was developed at NASA-Lewis, and is described in reference 2. Briefly this theory determines the mosture, thermal and mechanical load (hygrothermomechanical) response of a composite structure by integrating composite micro and macro mechanics, combined-stress failure criteria, laminate theory and advanced structural mechanics analysis programs. This integrated theory and other recent developments were used to predict the effects of hygrothermal environments on the properties of TFT/epoxy (TFT/E) and TFT/polyester (TFT/P) composite laminates and thereby assess their behavior in these environments. Comparisons of experimental data versus prediced TFT composite properties, based on hygrothermomechanical analysis, are presented and discussed.

2.0 COMPOSITE MATERIALS AND TEST SPECIMENTS

The composite lamintes evaluated in this report were fabricated under a DOE/NASA Contract for the design and fabrication of 60-foot fiberglass wind turbine blades (ref. 3). One of the tasks in this contract was to design and make flat TFT laminates for the preparation of test specimens to provide baseline static and cyclic fatigue properties for the design of future TFT fiberglass blades. The preparation and testing of the TFT specimens was accomplished under a related DOE/NASA contract (ref. 1).

2.1 TFT Laminate and Specimen Description

The transverse filament tape (TFT), used to make laminates, was in the form of 7-inch wide tape made from transverse bundles of E-glass fibers. The fiber bundles were supported by continuous carrier threads running transverse to the glass fiber bundles. The flat TFT laminates were made by wrapping resin-impregnated TFT materials over a rotating flat mandrel as shown schematically in figure 1. The TFT tape materials were wound using a 3-inch overlap, the same overlap used for construction of the 60-foot Mod-OA (200 kW wind turbine with a 120 ft diam rotor) blades (ref. 3).
Balanced symmetric laminates were made using two differnt winding patterns or ply configurations, as shown on table I. Winding Patern 1 was a 0° and 90° (0/90) laminate configuration and simulated the pattern used for the fabrication of the experimental 150-foot TFT fiberglass wind turbine blade (ref. 4). Winding Pattern 2 was a 0°, 90°, and +45° (0/90/+45) laminate configuration used for the fabrication of the 60-foot TFT Mod-OA blades. The TFT laminates also contain longitudinal filament tape (LFT) for compaction of the TFT plies and biased filament tape (BFT) for torsional stiffness in accordance with the blade design requirements.
TFT laminates were made using Winding Patterns 1 and 2 and an epoxy resin that was used for the fabrication of the 60 and 150 foot blades. TFT laminates were also made using Winding Pattern 2 and a low-cost polyester resin system.
After the laminates were wound on the mandrel, the mandrel and the uncured TFT composite windings were removed from the winding machine and sandwiched between two flat caul plates supported on a fixture. The uncured laminates were cut around the ends of the mandrel at this time to preclude the formation of curvature in the laminate during curing

The fixture was placed in an oven held at 200° F. Pressure was applied to the caul plate/laminate assembly by using a vacuum bag system that simulated the vacuum compaction used for fabrication of the 60-foot blades. After curing of the flat laminates was completed, the laminates were trimmed and subjected to an ultrasonic C-scan inspection. The results of the ultrasonic tests indicated that the laminates were of good quality and were suitable for the preparation of specimens.

2.2 Test Speciment Geometry

The laminates were cut into tension, compression, and interlaminar shear specimens in accordance with the specimen geometry shown in figure 2. The tension specimen shown in figure 2 is a straight-sided, flat specimen similar to the type used for the testing of advanced composite materials. Fiberglass doubler tabs were adhesively bonded to both sides of the specimens. The specimens were environmentally conditioned and then equipped with foil-type strain gages located at the center of the specimens.

2.3 Environmental Conditioning of Specimens

The environmental conditioning of specimens was accomplished as follows: For the room temperature dry condition (RTD), specimens were dried in an oven at 120° F for 6 hours, cooled to room temperature (70° F) and held in a laboratory-type desicator until ready for testing. Both static and cyclic fatigue tests were conducted in the RTD condition.

Wet conditions were attained by placing RTD-conditioned specimens in an oven at 120° F., and suspending but not immersing them over water for a period of 500 hours. One series of specimens was wet conditioned for a period of 4,000 hours. The weight gain after 500 hours was negligible, while the weight gain after the 4,000 hour exposure was about 2-percent by weight.

Environmental control during the static tests was accomplished by using an enclosed oven with a pan of water at the bottom to provide moisture. The wet fatigue tests were conducted in a enclosed environmental chamber. A detailed description of this chamber and the technique for testing multiple specimens simultaneously are presented in reference 5.

3.0 STATIC AND CYCLIC FATIGUE TESTING AND RESULTS

The static and cyclic fatigue test program is summarized in table II. The cyclic fatigue test schedule included R-values (ratio of min. to max. cyclic stress) ranging from 0 to -1.0. Because of the compressive stress imposed during the reversed portion of the tension test, the cyclic fatigue specimens were supported to prevent buckling by using bending stabilization fixtures. As noted in a previous section, the cyclic load (fatigue) tests were conducted in an environmental chamber that had the capability of testing five specimens simultaneously. Figure 3 shows a view of the test chamber with the top cover removed. The fixtures for multiple specimen testing can be seen inside the chamber. Figure 4 shows a view of the multiple specimen testing chain equipped with individual specimen stabilization fixtures.

Fan-induced airflow was provided across the specimens during cyclic fatigue testing at 30 Hz to control specimen temperatures. Specimen temperatures did not exceed 78° F for ambient conditions and 120° F for the elevated temperature/humidity condition.

3

3.1 Static Test Results

A summary of the average mechanical properties of the three TFT lami-
nate types is listed in table III. Observations derived from the test
results are as follows:

1.   Tensile and compression strengths of the TFT/epoxy composites with
Winding Pattern 1 are about 10-percent higher than the Winding Pattern 2
TFT/epoxy composites.

2.   The tensile and compressive moduli of the Winding Pattern 1 TFT/epoxy
composites are about 20-percent higher than the Winding Pattern 2 TFT/epoxy
composites as expected since Winding Pattern 2 has ±45-degree plies in
addition to 0/90 degree plies.

3.   No significant difference in interlaminar shear strength was noted
between resin systems and winding patterns.

4.   The tensile and compressive strengths of the TFT/ployester composites
were slightly lower than the Winding Pattern 1 TFT/epoxy composites. The
moduli of the TFT/polyester composites were closer to the moduli values for
the Winding Pattern 2 TFT/epoxy composites.

5.   The static strengths of the TFT/polyester composites are higher than
the corresponding strengths of the TFT/epoxy composites having the same
winding pattern.

6.   There appear to be no significant differences between wet and dry
strengths and moduli for the Winding Pattern 1 TFT/epoxy composites. There
appears to be a mixed behavior for Winding Pattern 2 TFT/epoxy composites,
but on an overall basis there is an insignificant difference between wet and
dry strength values.

7.   The wet interlaminar shear strengths for both winding patterns of the
TFT/epoxy composites were significantly higher than the corresponding dry
values.

8.   There was about a 25-percent decrease in the strengths of the
TFT/polyester composites which were exposed for 4,000 hours at 98-percent
relative humidity, compared to the corresponding dry strength properties

9.   The composite moduli (dominated by longitudinal fiber properties) were
not significantly affected by moisture.

Typical views of factured specimens are shown in figures 5 to 7.

3.2 Cyclic Fatigue Test Results

A summary of the tension-tension stress versus number of cycles to
failure (S-N) curves (R=0) for the Winding Patterns 1 and 2 TFT/epoxy com-
posites are shown in figures 8 and 9, respectively. Some reduction in the
wet cyclic fatigue strengths was indicated for the Winding Pattern 1
TFT/epoxy composites. The wet cyclic fatigue strengths were not determined

for all values of stress for the Winding Pattern 2 TFT/epoxy composites, but the values obtained for a 14.5 ksi stress range appeared to be part of the same S-N (stress versus number of cycles) curve. Thus the fatigue data for both dry and hygrothermal cases appear to coalesce at high fatigue cycles (N greater than 10^6).

The cyclic fatigue lines are plotted in figure 10 for various values of the stress range (S-max. - S-min.) for the Winding Pattern 1 TFT epoxy composites. The data in figures 8 to. 10 were used to construct a modified Goodman plot shown in figure 11. The modified Goodman plot can be used for the design of TFT fiberglass wind turbine blades and other structural components. The curves shown in figure 11 are similar to those obtained for other common aerospace materials such as metals, plastics, and composites.

4.0 HYGROTHERMOMECHANICAL ANALYSIS, RESULTS AND COMPARISONS

A hygrothermomechanical analysis was performed to predict the environmental effects on the properties of the TFT composites. The predictions are based on the theories described in reference 2. The predictions include unidirectional properties of the TFT, properties of the laminates with Winding Patterns 1 and 2, thermal and hygral ply stresses, laminate strength, fatigue strength and attendant environmental effects. These are described below.

4.1 Unidirectional Composite Properties

The predicted properties of the unidirectional composites needed for hygrothermomechanical analysis (NO.transverse filaments) are summarized in table IV for TFT/ epoxy (TFT/E) and TFT/polyester (TFT/P). These properties are for RTD conditions. The properties in this table were not previously available. They were determined analytically from the measured properties given in table III and composite micromechanics using typical properties for E-glass fiber, epoxy and polyester resin, for example, thermal expansion coefficients, moisture expansion coefficients, tensile strength, and glass transition temperature. The properties used from table III were modulus, Poisson's ratio, tensile strength, compressive and interlaminar shear strengths for Winding Pattern 1 only These properties were used with composite micromechanics to back calculate the corresponding matric (epoxy and polyester) properties and the fiber volume ratio. Subsequently, these resin properties were used with composite micromechanics to determine the first 15 properties listed in table IV. The ply thickness was determined from the measured laminate thickness and the winging patterns summarized in table I.

4.2 TFT Composite Properties

The TFT composite properties used in the hygrothermomechanical analysis are summarized in table V. The properties listed in this table were determined using laminate theory (ref. 6) and the unidirectional composite properties in table IV. The predicted modulus (E_{cxx}) values in table V are within 7-percent of the average of the corresponding moduli in table III. This is considered to be a very good agreement since most of the unidirectional properties needed for these calculations were determined using composite micromechanics, as mentioned previously. The predicted

5

values of the Poisson's ratios in table V are about 30-percent smaller than the average of the corresponding values in table III. This indicated that the 0° plies and the +45° plies do not provide as much transverse restraint in a uniaxial test compared to the restraint inherent in the laminate theory.

4.3 Ply Thermal Stresses

The ply thermal stresses were determined using laminate theory. Laminate theory requires ply properties, composite (laminate) properties and the respective change in temperature (ΔT). The ply and laminate properties are tabulated in tables IV and V, respectively. The change in temperature (ΔT) was the difference in use-temperature (120° F) minus the cure temperature (70° F) or ΔT equals 50° F (120° - 70° F) for the environmental conditions in table III. Of the three ply thermal stresses (longitudinal, transverse, and shear), the transverse is usually the most critical since this stress causes transply cracks when it is tensile. The transverse ply thermal stresses were compressive in the 0°, 90°, and +45° plies for both composite systems and for both winding patterns. The maximum magnitude in the +45° plies was about -600 psi which was only about 3-percent of the corresponding ply transverse compressive strength ($S_{\ell22c}$ = 20,000 psi) in table IV. The conclusion from the thermal stress analysis is that the thermal stresses are negligible in TFT/E and TFT/P laminates for a temperature change of 50° F.

4.4 Ply Hygral Stresses

The ply hygral stresses were also determined using laminate theory with ply properties (table IV), laminate properties (table V) and the respective moisture change. The moisture change equals the moisture pick-up from a reference condition, usually room temperature dry. The moisture change is about 2-percent for the environmental conditions in table III. The ply transverse hygral stresses are the most critical since these could cause transply cracks, as was the case for the thermal stresses. The predicted ply transverse hygral stresses are compressive and about -1,500 psi which is about 8-percent of the corresponding ply transverse compressive strength $S_{\ell22c}$ =20,000 psi) in table IV. The conclusion from the ply hygral stress analysis is that the hygral stresses are negligible in both winding patterns and both composite systems for the 2-percent moisture environmental condi- tion. It is interesting to note that the ply hygral stresses are about twice the corresponding thermal stress.

4.5 Laminate Static Strength

The laminate static strength was predicted using laminate theory in conjunction with ply stress influence coefficients (ref.7). Both ply (table IV) and laminate (table V) properties are needed to determine laminate strength using the ply stress influence coefficients. Laminate strength is determined for three different conditions: (1) room temperature dry (RTD), (2) with a hygrothermal environment (HT-ENV.) and (3) hygrothermally degraded (HT-degraded). Laminate strengths were determined for TFT/E Winding Patterns 1 and 2, and TFT/P for Winding Pattern 2 (corresponding to the experimental data in table III). The HT-degraded properties were determined using the procedure (ref.8): (1) an empirical equation to

estimate the glass transition temperature of a wet composite (T_{gw}) is as follows:

$$T_{gw}/T_{go} = 0.01 M^2 - 0.1M + 1 \tag{1}$$

where T_{gt} is the glass transition temperature of the dry (reference) composite and M is the moisture in percent by weight; and (2) an empirical equation to estimate the HT-degraded "resin-controlled" property (P_{HT}) is as follows:

$$P_{HT}/P_0 = \left\{ (T_{gw} - T)/(T_{go} - T_0) \right\}^{1/2} \tag{2}$$

where P_0 is the composite "resin-controlled" property at reference conditions, T is the use-temperature, and T_0 is the temperature at which P_0 was measured.

The glass transition temperature of the dry composite (T_{go}) was determined experimentally to be about 230° F for both TFT/E and TFT/P composites. Using T_{go} = 230° F and M = 2-percent in equation (1), the glass transition temperature of the wet composite, T_{gw} = 193° F. Using T_{go} = 230° F, T_{gw} = 193° F, T = 120° F (test temperature), and T = 70° F, the HT-degraded ratio for "resin controlled" composite properties (P_{HT}/P_0) = 0.68. This is the required value to determine the degree of hygrothermal degradation for the three different conditions enumerated previously.

Comparisons of the tension, compression, and interlaminar shear strengths for the TFT/E Winding Pattern 1 are shown in figure 12 in bar-chart form. similar comparisions for the TFT/E Winding Pattern 2 are shown in figure 13 and for the TFT/P Winding Pattern 2 in figure 14. The agreement between measured data and predicted results is excellent. In addition, the predicted HT-degraded properties are somewhat smaller than the experimental data except for the interlaminar shear, figure 14, for which no adequate explantation is available as of this writing. Important conclusions from the strength predictions and comparisons area; (1) the concepts/equations developed previously for hygrothermal effects are applicable to TFT/E and TFT/P laminates as well, (2) the predicted HT-degraded properties for tensile and compressive strengths for the TFT-composites are conservative as compared with measured data. This is significant because using the HT-degraded properties for design allowables should lead to conservative designs, and (3) the ply stress influence coefficients are an effective means to determine laminate strengths when only a minimum of measured data is available.

4.6 Fatigue Life

Fatigue life (S_N) of composites was predicted using the empirical equation described in reference 9. This empirical equation, expressed here in slightly different form to account for laminate degraded strength as determined previously, is as follows:

$$S_N/S_1 = 1.0 - B \, Log \, N \tag{3}$$

7

where S_n denotes the fatigue life for N cycles, S_1 denotes the static strength which includes HT-degradation and N denotes the number of fatigue cycles. The coefficient B depends on the composite system and the dominant fracture mode. For longitudinal fracture in fiberglass composites, B is about 0.13 (ref. 9). Obviously, this coefficient can readily be adjusted to obtain better correlation between experimental data and predicted results. Using B = 0.13 in equation (3) and respective strengths from figures 12 and 13, the predicted fatigue life curves are plotted: (1) in figure 15 for TFT/E Winding Pattern 1, (2) in figure 16 for TFT/E Winding Pattern 2, and (3) in figure 17 for TFT/E Winding Pattern 1 and different R-ratios.

The predicted fatigue results are in good agreement with the dry data for all the cases in figures 15 to 17. The predicted curves underestimated the fatigue life for both dry and hygrothermal data at high fatigue cycles (10^6 cycles and greater). The HT-degraded curve over-estimated the fatigue life of the TFT/E Winding Pattern 1 composite especially at low fatigue cycles (10^6 and lower), figure 15. A higher value for the B coefficient would need to be used to obtain better correlation for the hygrothermal case. It appears from the experimental data in figures 15 through 17 that a bilinear fit would be more appropriate. This can be done by using two different values for the B coefficient in equation (3), one for the range where N is less or equal to 10^6 cycles, and a smaller one for the range where N is greater than 10^6 cycles.

The significant conclusion from the fatigue life prediction and comparisons is that the fatigue life of TFT composite laminates can be adequately predicted for lives up to 10^6 cycles, using the recently developed hygrothermomechanical theory and life/durability procedures. This conclusion/finding should lead to considerable reduction in experimental effort for determining the fatigue life of TFT composites for structural applications up to 10^6 cycles, however selective testing for higher numbers of cycles may still be necessary.

Taken collectively, the hygrothermal analysis, results and comparisons described herein demonstrated that: (1) composite mechanics can be used effectively to analyze and design TFT composite structural components, (2) combination of composite mechanics with limited experimental data can be a reliable and cost-effective way to characterize new composite system, and (3) the methodology is available for the analysis and preliminary design of TFT composite structural components in hygrothermomechanical environments.

5.0 CONCLUSIONS

The following conclusions are derived from the results and comparisons of the experimental static and cyclic fatigue testing program, as well as the hygrothermomechanical analysis of the TFT (epoxy and polyester (0/90) and (0/+45/90)) balanced symmetric angleplied laminate behavior.

1. The effect of elevated temperature and moisture on the static tensile and compressive strengths of the TFT/E composites is not significant for the conditions studied.

2. The elastic moduli of these angleplied composites are not affected by temperature, humidity, load direction (tension or compression), or by resin type.

8

3.   Cyclic fatigue data show that moisture and temperature have an effect on the fatigue behavior of the Winding Pattern 1 TFT/E composites (0/90). However moisture and temperature have no affect on the cyclic behavior of the Winding Pattern 2 TFT/E composites (0,90/±45).

4.   The hygrothermomechanical integrated theory predicts results which are in good agreement with measured data for elastic and strength properties, while the predicted hygrothermal ply stresses are insignificant compared to corresponding ply strength.

5.   The life/durability theory adequately predicts the fatigue life of the TFT composites up to 10^6 cycles, though the correlation coefficient may need to be adjusted for the 120° F, 98-percent relative humidity data for the TFT/E Winding Pattern 1 composite.

6.   Collectively, the hygrothermal analysis, results and comparisons demonstrate that the methodology is available for the analysis and preliminary design of TFT composite structural components in hygrothermomechanical environments.

6.0 REFERENCES

1.   K.E. Hofer, and L.C. Bennett, "Fatigue Testing of Low-Cost Fiberglass Composite Wind Turbine Blade Materials," IITRI-M06066-22, IIT Research Institute, Chicago, IL, NASA CR-165566, November 1981. (DOE/NASA/0182-1.)

2.   C.C. Chamis, R.F. Lark, and J.H. Sinclair, in "Advanced Composite Materials - Environmental Effects," J.R. Vinson, Editor, ASTM STP-658, pp. 160-192, American Society for Testing and Materials, New York, 1978.

3.   O. Weingart, "Design, Evaluation and Fabrication of Low-Cost Composite Blades for Intermediate-Size Wind Turbines," SCI-81520, Structural Composites Industries, Inc., Azusa, CA, DOE/NASA/0100-1, NASA CR-165342, Sept. 1981.

4.   H.W. Gewehr, "Design, Fabrication, Test and Evaluation of a Prototype 150-Foot Long Composite Wind Turbine Blade," R-1574, Kaman Aerospace Corp., Bloomfield, Conn., DOE/NASA/0600-79/1, NASA CR-159775, Sept. 1979.

5.   K.E. Hofer, and J. Jollay, in "Fibrous Composites in Structural Design," E. Lenoe, O.W. Oplinger, and J.J. Burke, Editors, pp. 831-845, Plenum Press, New York, 1980.

6.   C.C. Chamis, Comput. Struct. (3) 467-482 (1973).

7.   C.C. Chamis, in "Rising to the Challenge of the '80s," pp.12-A1 to 12-A10, Society of the Plastics Industry, Inc, New York, 1980.

8.   C.C. Chamis, "Designing With Fiber-Reinforced Plastics (Planar Random Composites), "NASA TM-82812, 1982.

9.   C.C. Chamis, and J.H. Sinclair, "Durability/Life of Fiber Composites in Hygrothermomechanical Environments," NASA TM-82749, 1981.

TABLE I. - LAYUP SCHEDULE FOR TFT LAMINATE WINDING PATTERNS

Winding Pattern	Ply Designation	Ply Angle[d] (Degrees)	Number of Plies	Total Number of Plies
1	TFT[a]	0°	5[e]	
	LFT[b]	90°	1	
	TFT	0°	5	
	LFT	90°	1	
	TFT	0°	5	
	LFT	90°	1	
	TFT	0°	5	
	LFT	90°	1	
	TFT	0°	5	29
2	TFT	0°	5	
	LFT	90°	1	
	BFT[c]	±45°	1[f]	
	LFT	90°	1	
	TFT	0°	5	
	LFT	90°	1	
	TFT	0°	5	
	LFT	90°	1	
	BFT	±45°	1	
	LFT	90°	1	
	TFT	0°	5	27

[a]Transverse filament tape, 7 oz/yd^2, 7 in. wide.

[b]Longitudinal filament tape, 10 oz/yd^2, 3 in. wide.

[c]Biased filament tape, 15 oz/yd^2, 7 in. wide.

[d]To the principal structural load direction, i.e., along the length of the blade.

[e]Although five successive passes of the TFT were made, the tape was layed down with a 4-inch overlap, thus producing a total of approximately 2-1/3 layers per pass; thus, the ratio of 0° filaments to 90° filaments for Winding Pattern 1 is approximately 15:1.

[f]Both 45° plies are incorporated into one "working" ply.

10

TABLE II. - STATIC AND FATIGUE TEST PLAN

STATIC TESTS

Material Type	Winding Pattern	Preconditioning	Test Conditions	Minimum Number of Specimens Per Property		
				Tension	Compression	Shear
TFT/epoxy	1	dry[a]	dry	5	5	5
		wet[b]	wet	5	5	5
	2	dry	dry	5	5	5
		wet	wet	5	5	5
TFT/polyester	2	dry	dry	5	5	5
		wet	wet	5	5	5

FATIGUE TESTS

Material Type	Test Conditions Temperature/Humidity	Number of Specimens Per R[c] Ratio				
		R=0	R=-0.1	R=-0.25	R=-0.5	R=-1.0
TFT/epoxy; Winding Pattern 1	70°F/50% RH	12	8	5	5	5
	120°F/98% RH	5	5	5	5	5
TFT/epoxy; Winding Pattern 2	70°F/50% RH	12	5	5	5	5
	120°F/98% RH	5	5	5	5	5
TFT/polyester; Winding Pattern 2	70°F/50% RH	5	5	-	-	5
	120°F/98% RH	5	5	-	-	5

[a] Dry = 70°F, Relative Humidity (RH) = 50%.

[b] Wet = 120°F, RH = 98% for 500 hours.

[c] R = Ratio of minimum stress per cycle to maximum stress per cycle.

Epoxy resin components - DER-332 with RD-2 reactive diluent and Tonox 6040 hardener.

Polyester resin components - Polylite-AZ7623 catalyzed with cumenehyperoxide and Percodox 16N.

A thixotropic additive (1.5% Cab-o-Sil) was mixed with both resins to provide the thickened resin used for fabrication of the 60-ft. blades. This additive was included in the resin system to control resin flow during blade fabrication.

11

TABLE III. - SUMMARY OF STATIC TEST RESULTS

Material[a]	Load Type	Material Condition	Strength ksi	Modulus of Elasticity 10^6 psi	Poisson's Ratio
A	Tension	RTD[b]	67.2	4.63	0.284
		wet[c]	69.0	4.27	0.243
	Compression	RTD	55.6	4.61	0.300
		wet	55.1	4.49	- -
	Interlaminar Shear	RTD	6.3	- -	- -
		wet	10.8	- -	- -
B	Tension	RTD	59.9	3.85	0.312
		wet	56.0	3.44	0.331
	Compression	RTD	48.6	3.67	0.318
		wet	51.9	4.06	- -
	Interlaminar Shear	RTD	7.2	- -	- -
		wet	10.6	- -	- -
C	Tension	RTD	64.7	3.64	0.281
		wet	63.9[d]	3.81	0.299
	Compression	RTD	49.7	4.28	0.252
		wet	48.2	4.11	0.259
	Interlaminar Shear	RTD	10.5	- -	- -
		wet	9.2	- -	- -

[a] Material A = Winding Pattern 1 TFT/E composite.
  Material B = Winding Pattern 2 TFT/E composite.
  Material C = Winding Pattern 2 TFT/P composite.

[b] RTD = room temperature dry (70°F), and 50% relative humidity.

[c] West = 120°F and 98% relative humidity for 500 hours.

[d] Additional information at 4,000 hours exposure indicates that the tensile strength drops to 46.4 ksi.

TABLE IV.   SUMMARY OF PREDICTED UNIDIRECTIONAL COMPOSITE PROPERTIES

PROPERTY	SYMBOL	UNITS	TFT/EPOXY.	TFT/POLYESTER
Fiber Volume Ratio	k_f	-	0.47	0.43
Density	ρ_l	lb/in³	0.066	0.064
Long. Modulus	E_{l11}	msi	5.1	4.7
Transv. Modulus	E_{l22}	msi	1.3	1.2
Shear Modulus	G_{l12}	msi	0.53	0.51
Major Poisson's Ratio	ν_{l12}	-	0.28	0.29
Long. Thermal Exp. Coef.	α_{l11}	μin/in°F	4.3	4.4
Transv. Thermal Exp. Coef.	α_{l22}	μin/in°F	17.7	19.0
Long. Moisture Exp. Coef.	β_{l11}	in/in/ %M	0.00014	0.00016
Transv. Moisture Exp. Coef.	β_{l22}	in/in/ %M	0.00113	0.00125
Long. Tensile Strength	S_{l11T}	ksi	78	83
Long. Compres. Strength	S_{l11C}	ksi	62	64
Transv. Tensile Strength	S_{l22T}	ksi	5	5
Transv. Compres. Strength	S_{l22C}	ksi	20	20
Interlaminar Shear Strength	S_{l12S}	ksi	6	8
Ply Thickness	t_l	in	0.017	0.017

Note: These properties were predicted using composite micromechanics and nominal constituent material properties.

TABLE V. PREDICTED ANGLEPLY COMPOSITE PROPERTIES

Property	Symbol	Units	TFT/Epoxy		TFT/Polyester	
			W.P. 1[a] (0/90)	W.P. 2[a] (0/90/+45)	W.P. 1 (0/90)	W.P. 2 (0/90/+45)
Fiber Volume Ratio	k_f	–	0.47	0.47	0.43	0.43
Density	ρ_c	lb/in^3	0.066	0.066	0.064	0.064
Moduli						
Along Load Direct.	E_{cxx}	msi	4.60	4.03	4.24	3.72
Transv. to Load Direct.	E_{cyy}	msi	1.83	2.08	1.70	1.92
In-Plane Shear	G_{cxy}	msi	0.53	0.67	0.51	0.62
Major Poisson's Ratio	ν_{cxy}	–	0.20	0.23	0.21	0.24
Thermal Exp. Coef.						
Along Load Direct.	α_{cxx}	µin/in/°F	4.5	4.5	4.6	4.6
Transv. to Load Direct	α_{cyy}	µin/in/°F	6.8	5.9	7.1	6.1

[a] W.P. 1,2 = Winding Pattern 1,2

Note: The properties in this table were predicted using laminate theory and the unidirectional composite properties in Table IV.

14

TI I, II I, AND/OR
BI T ROI I S
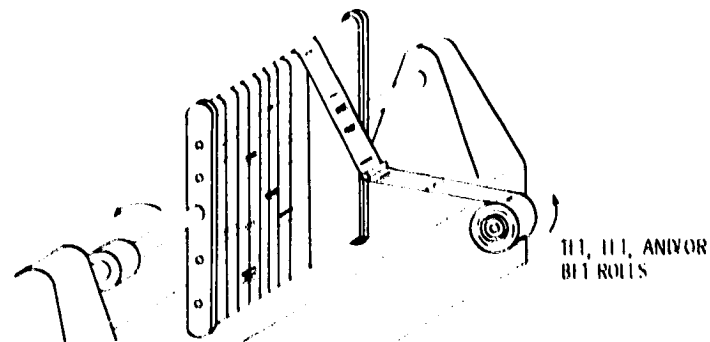
Figure 1. - Fabrication of flat TI I laminates.

ELECTRIC RESISTANCE FOIL STRAIN GAGES

FIBERGLASS TAB (0.06)
STATIC AND FATIGUE TEST SPECIMEN

FULL LAMINATE
THICKNESS

STATIC COMPRESSION SPECIMEN

P - LOAD

FULL LAMINATE
THICKNESS

INTERLAMINAR SHEAR SPECIMEN   DIMENSIONS IN in.
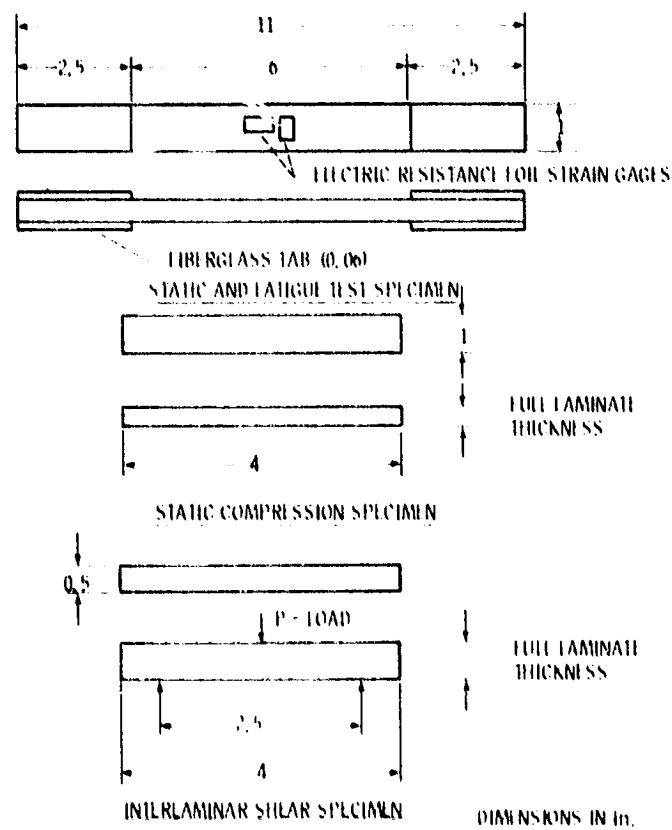
Figure 2. Test specimen geometry.
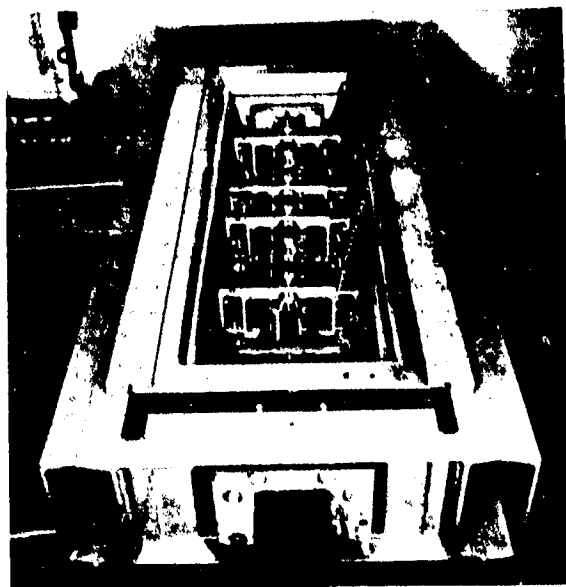
Figure 3. - Environmental test chamber for multiple specimen testing.
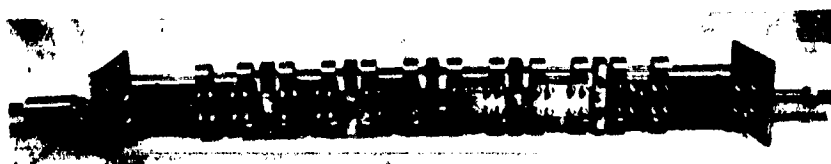
Figure 4. Multiple specimen loading chain.

WINDING PATTERN 2   WINDING PATTERN 1

Figure 5. - Typical fracture appearance of winding pattern nos. 1 and 2 specimens
subjected to static compression loading.

WINDING PATTERN 1   WINDING PATTERN 2   WINDING PATTERN 3

Figure 6. - Typical fracture appearance of specimens subjected
to static tension loading.

Figure 7. - Typical fracture appearance of winding pattern no. 2
specimens subjected to full-reversed cyclic fatigue loading.
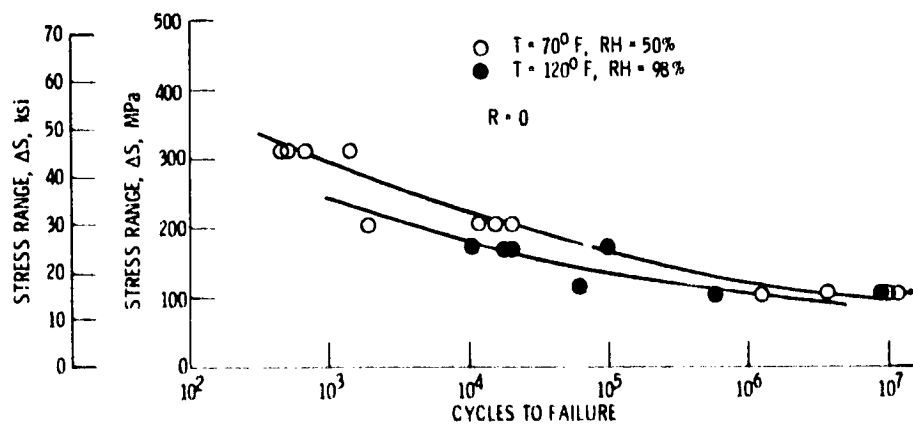
Figure 8. - S-N fatigue life diagram for winding pattern 1 TFT/EPOXY composites.
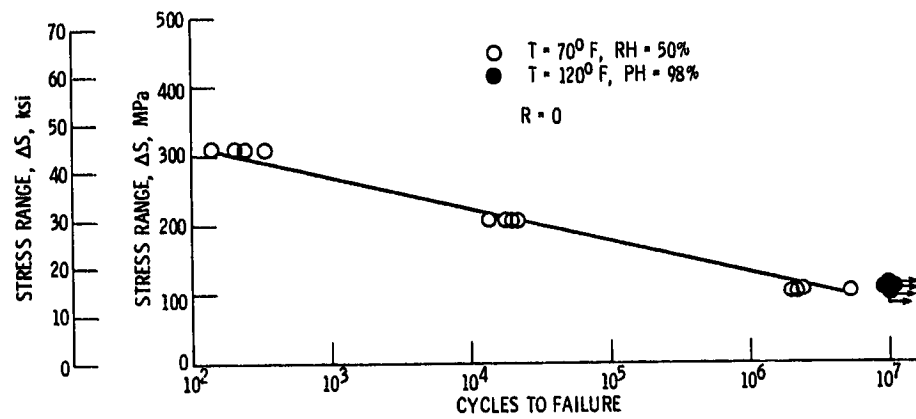
Figure 9. - S-N fatigue life diagram for winding pattern 2 TFT/EPOXY composites.
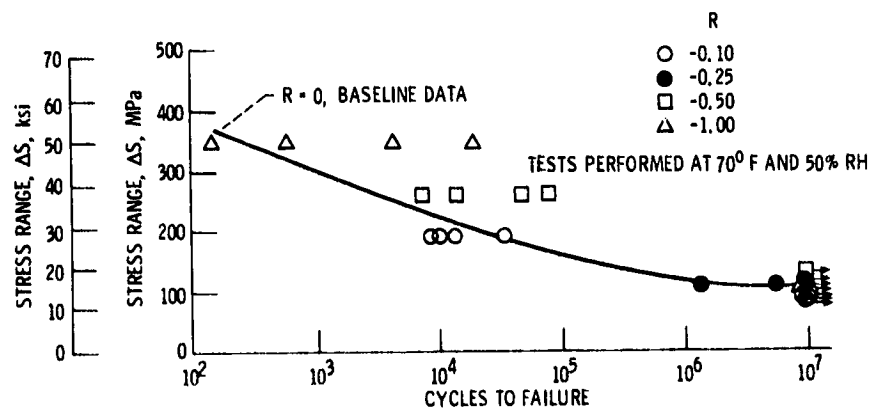
Figure 10. - Effect of mean stress on fatigue endurance for winding pattern 1 TFT/EPOXY composites.
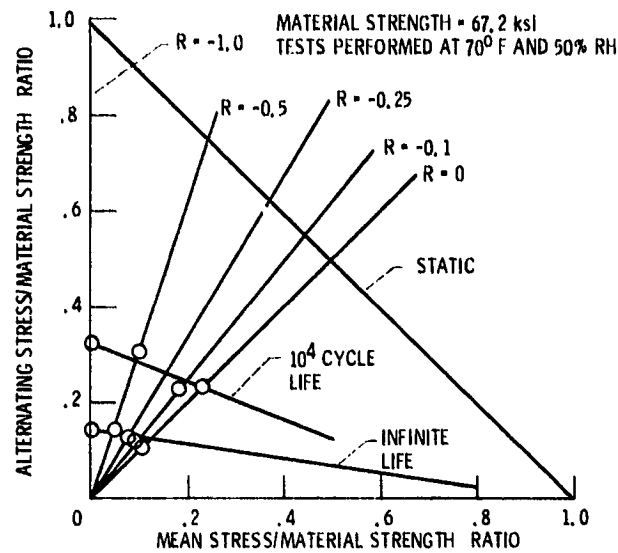
Figure 11. - Modified Goodman diagram illustrating the effect of mean stress on the behavior of winding pattern 1 TFT/EPOXY composites.
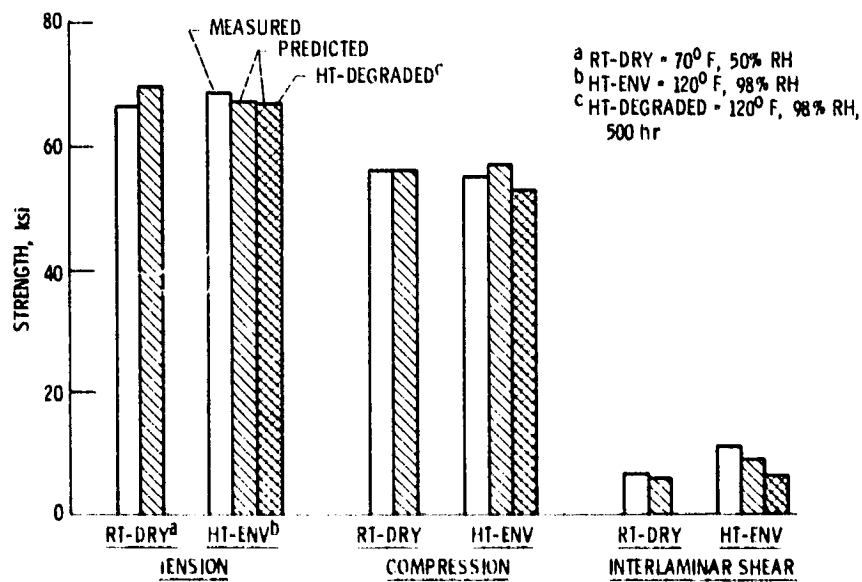
Figure 12. - Strength comparisons - TFT/EPOXY winding pattern 1 (0°/90°).
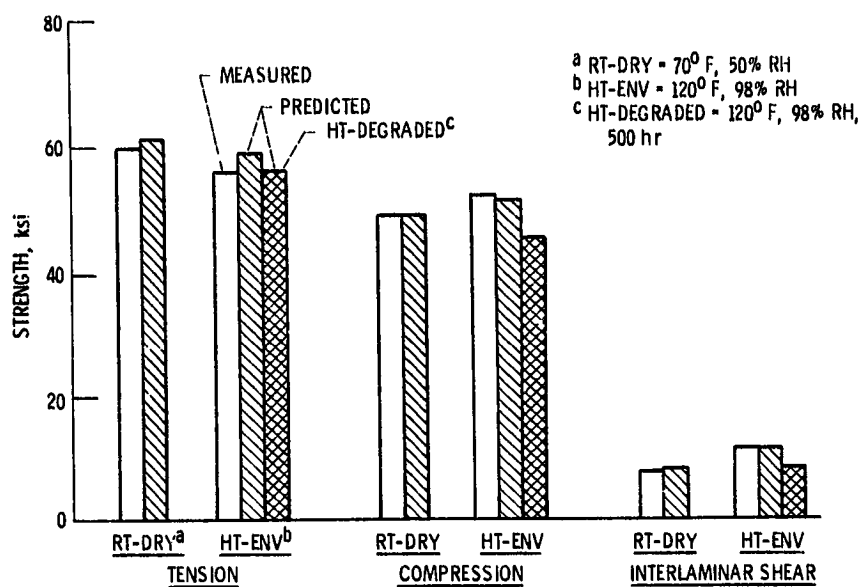
Figure 13. - Strength comparisons - TFT/EPOXY winding pattern 2 (0^0/90^0/±45^0).
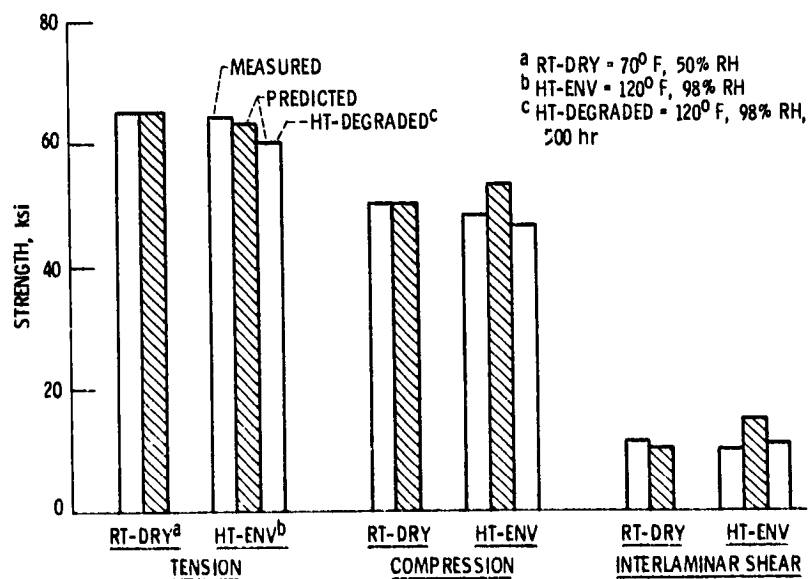
Figure 14. - Strength comparisons - TFT/polyester winding pattern 2 (0^0/90^0/±45^0).
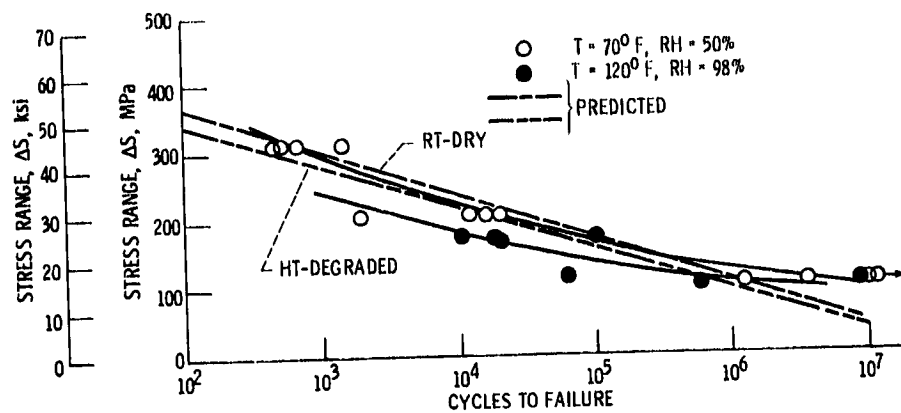
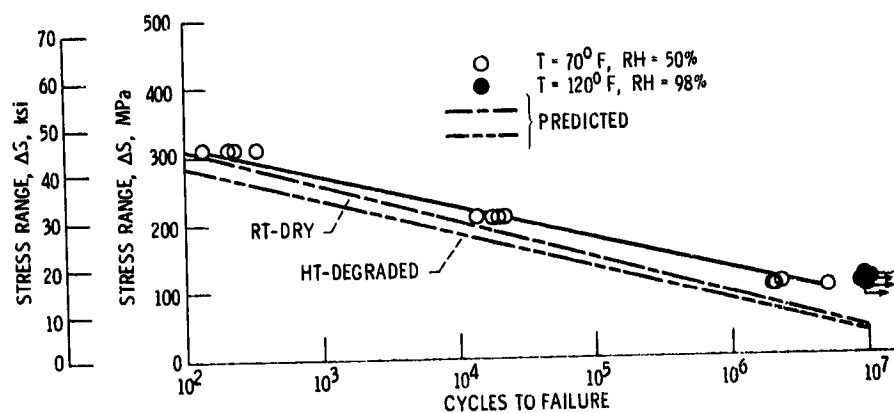Figure 15. - Comparison of S-N fatigue life diagram for winding pattern 1 TFT/EPOXY composites (R = 0).

Figure 16. - Comparison of S-N fatigue life diagram for winding pattern 2 TFT/EPOXY composites (R = 0).
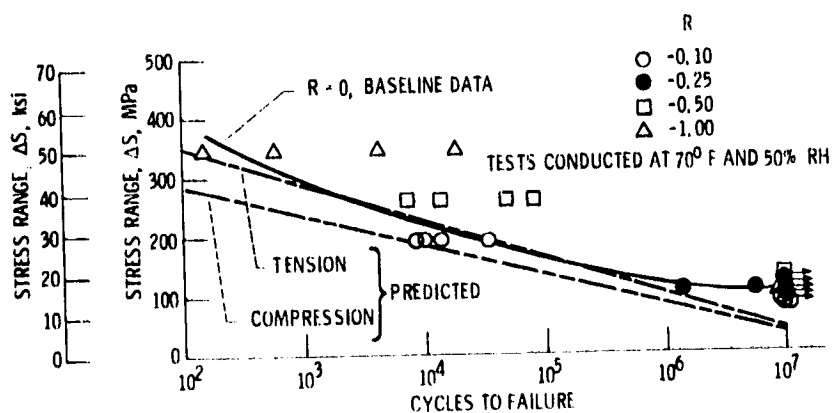

Figure 17. - Comparison of effect of mean stress on fatigue endurance for winding pattern 1 TFT/EPOXY composites.